

Cite this: *Soft Matter*, 2011, **7**, 11232www.rsc.org/softmatter**PAPER**

Phase behaviour and structure of zwitanionic mixtures of perfluorocarboxylates and tetradecyldimethylamine oxide—dependence on chain length of the perfluoro surfactant[†]

Katharina Bressel,^{*a} Sylvain Prevost,^{ab} Marie-Sousai Appavou,^c Brigitte Tiersch,^d Joachim Koetz^d and Michael Gradzielski^{*a}

Received 7th April 2011, Accepted 2nd August 2011

DOI: 10.1039/c1sm05618b

Phase behaviour and the mesoscopic structure of zwitanionic surfactant mixtures based on the zwitterionic tetradecyldimethylamine oxide (TDMAO) and anionic lithium perfluoroalkyl carboxylates have been investigated for various chain lengths of the perfluoro surfactant with an emphasis on spontaneously forming vesicles. These mixtures were studied at a constant total concentration of 50 mM and characterised by means of dynamic light scattering (DLS), electric conductivity, small-angle neutron scattering (SANS), viscosity, and cryo-scanning electron microscopy (Cryo-SEM). No vesicles are formed for relatively short perfluoro surfactants. The extension of the vesicle phase becomes substantially larger with increasing chain length of the perfluoro surfactant, while at the same time the size of these vesicles increases. Head group interactions in these systems play a central role in the ability to form vesicles, as already protonating 10 mol% of the TDMAO largely enhances the propensity for vesicle formation. The range of vesicle formation in the phase diagram is not only substantially enlarged but also extends to shorter perfluoro surfactants, where without protonation no vesicles would be formed. The size and polydispersity of the vesicles are related to the chain length of the perfluoro surfactant, the vesicles becoming smaller and more monodisperse with increasing perfluoro surfactant chain length. The ability of the mixed systems to form well-defined unilamellar vesicles accordingly can be controlled by the length of the alkyl chain of the perfluorinated surfactant and depends strongly on the charge conditions, which can be tuned easily by pH-variation.

1. Introduction

Mixtures of cationic or zwitterionic and anionic surfactants (catanionics or zwitanionics) have been studied intensively before, with a particular emphasis on catanionic surfactants.^{1–6} Such catanionic mixtures are well-known to form vesicles spontaneously, as shown for a variety of systems of single alkyl chain^{7–10} or double alkyl chain surfactants¹¹ and for these systems energetically stabilized vesicles are predicted on a theoretical basis.¹² In

addition, it is also possible to have entropic stabilisation of vesicles which can occur for bilayers with low bending rigidity.⁸ However, catanionics have a tendency for precipitation around equimolar mixing ratios. In contrast, mixtures of anionic and zwitterionic surfactants possess less synergistic interaction between the surfactant pairs, therefore are less prone to precipitation, but may also form vesicular systems.^{13–18} Especially for the case of mixing a zwitterionic hydrocarbon surfactant with an anionic perfluoro surfactant one may observe the formation of vesicles.

This is not surprising due to the fact that perfluoro surfactants are known to have a propensity for the formation of bilayers, due to their much bulkier and stiffer alkyl chains compared to hydrocarbon chains.^{19,20} Accordingly in recent investigations we have studied the phase behaviour of mixtures of the zwitterionic tetradecyldimethylamine oxide (TDMAO) and the anionic lithium perfluoroctanoate ($C_7F_{15}CO_2Li$), which show an extended range of formation of unilamellar vesicles,²¹ as well as the kinetics of their formation process, which proceeds via disk-like intermediates.^{17,22} Similar results have been observed for mixtures of TDMAO lithium perfluoroctanesulfonate (LiPFOS) by SANS.²³ The formation process via disc-like micelles has been well established for mixtures of surfactants above the cmc, while new investigations show that the

^aTechnische Universität Berlin, Institut für Chemie, Stranski Laboratorium für Physikalische und Theoretische Chemie, Sekr. TC7, Straße des 17. Juni 124, 10623 Berlin, Germany. E-mail: katharina.bressel@mailbox.tu-berlin.de; michael.gradzielski@tu-berlin.de

^bHelmholtz-Zentrum Berlin für Materialien und Energie, Lise-Meitner-Campus, Hahn-Meitner-Platz 1, 14109 Berlin, Germany

^cForschungszentrum Jülich, Jülich Center for Neutron Science at FRM2, Lichtenbergstraße 1, 85747 bei Garching, Germany

^dUniversität Potsdam, Institut für Chemie, Karl-Liebknecht-Straße 24–25, Haus 25, 14476 Golm/Potsdam, Germany

[†] Electronic supplementary information (ESI) available: Individual cmc and DLS measurements, pH measurements, theoretical background for SANS analysis, and additional parameters obtained from SANS. See DOI: 10.1039/c1sm05618b

mechanism proceeds *via* a torus-like state, if the anionic surfactant is below the cmc.²⁴ Generally, in these surfactant mixtures long-time stable unilamellar vesicles are formed spontaneously which do not precipitate. In comparison the corresponding catanionic mixtures with tetradecyltrimethylammonium bromide (TTABr) show a tendency for precipitation after some time. Accordingly zwitanionic surfactant mixtures are interesting as they allow for the formation of long-time stable unilamellar vesicles.

As a logical extension of these previous studies we were now interested in the precise effect of the molecular composition of the surfactant mixture in such systems on the ability for spontaneous formation of vesicles. The stability of formed vesicles should depend on the interaction between the surfactants which is controlled by the length of their alkyl chains and on the extent of attractive interaction between the head groups. To obtain a more general understanding on a molecular level we varied in this investigation in a systematic fashion the length of the perfluoro chain of the anionic surfactant. For that purpose we employed perfluorohexanoate and -heptanoate, and compared them to the formerly studied perfluoroctanoate. In addition, we investigated in this study the transfer from a zwitanionic system to a partially catanionic system by charging the TDMAO head group to a certain extent with HCl thereby changing the head group interactions in the mixture. From these variations we expect to obtain an insight into the effect of chain length and head group interactions on the ability of a given surfactant mixture to form vesicles.

2. Experimental

2.1. Materials

The tetradecyldimethylamine oxide (TDMAO) was kindly given by Stepan (Stepan Company, Northfield, Illinois, USA) as a 25% TDMAO solution in water named Ammonyx M. This solution was freeze-dried and used without further purification. The cmc measurements were done with TDMAO, kindly provided by Clariant (Germany), which was purified by recrystallizing twice from acetone. Both TDMAO batches (from Stepan and from Clariant) had very similar cmc values of 0.15 mM and 0.14 mM, respectively. Perfluorohexanoic acid ($C_5F_{11}CO_2H$, 97%), perfluoroheptanoic acid ($C_6F_{13}CO_2H$, 95%) and lithium hydroxide ($LiOH \cdot H_2O > 99\%$) were purchased from Fluka. Perfluoroctanoic acid ($C_7F_{15}CO_2H$, 96%) was purchased from Sigma-Aldrich. Deuterium oxide ($D_2O > 99.96\%$) was purchased from Eurisotop. All SANS samples were prepared using D_2O instead of H_2O , in order to have enhanced contrast conditions and low incoherent background. Hydrochloric acid was purchased from Sigma-Aldrich as a 0.5 N volumetric solution. All these substances were used as supplied. The characteristic parameters of the surfactants are summarized in Table 1. The perfluoro surfactant solutions were prepared by dissolving the acid in water and neutralizing with LiOH solution to the equivalence point. All surfactant solutions were prepared using Milli-Q water. The samples were prepared as mixtures of the stock solutions, homogenized by vigorous shaking by a vortex mixer, and then equilibrated at 25 °C.

2.2. Methods

2.2.1. pH-determination. The samples were equilibrated in a water bath at (25 ± 0.1) °C before the pH was measured at

room temperature without further temperature control with a Mettler Toledo MP 220 pH meter.

2.2.2. Determination of the critical micelle concentration (cmc)/electric conductivity. The critical micelle concentration was determined by measuring the electric conductivity of a sample during dilution with Milli-Q-water. This was done with a Titrando 836 (Metrohm AG) and the conductivity was measured at 25 °C by means of a conductometer 712 (Metrohm AG).

By plotting the conductivity *versus* the surfactant concentration two linear regions are observed (Figs. S.1 to S.7†). Those linear regimes were interpolated and the intersect marks the cmc. Usually the slope decreases when micelles are formed due to binding of counter ions to the micelles. However, in most micellar systems with an anionic perfluoro surfactant and TDMAO the slope increases above the cmc due to protonation of the TDMAO and the formation of hydroxide ions in the solution.

2.2.3. Viscosity. The viscosity was measured at (25±0.1) °C with an Ubbelohde-Viscosimeter (Schott 0a, recommended for 0.8–5 mm² s⁻¹) or an Ostwald-Viscosimeter (Schott 1c, recommended for 3–20 mm² s⁻¹). The values for the viscosity were determined from the average of three independent measurements.

2.2.4. Dynamic light scattering (DLS). DLS measurements were performed with an ALV/CGS-3 Compact Goniometer system with a 22 mW HeNe-Laser ($\lambda = 632.8$ nm) and employing a pseudo cross-correlation under a scattering angle of 90°. The samples were thermostatted at 25 °C in a toluene bath. Biphasic samples were homogenized before the measurement and measured as such. The analysis of the intensity correlation function was typically done with a cumulant fit (1) and in some cases with a bi-exponential fit (2):

$$\ln(g^{(2)}(\tau)) = A - 2\langle\Gamma\rangle\tau + 2\mu_2\tau^2 \quad (1)$$

$$g^{(2)}(\tau) = 1 + A_1 \cdot \exp(-\tau_1\Gamma_1) + A_2 \cdot \exp(-\tau_2\Gamma_2) \quad (2)$$

The translational diffusion coefficient D_T was calculated from the relaxation rate $\Gamma = D_T q^2$, where $q = 4\pi n/\lambda \sin(\theta/2)$ is the magnitude of the scattering vector with the refractive index n , the wavelength of the laser light λ , and the scattering angle θ . The hydrodynamic radius R_h was calculated from D_T by employing the Stokes-Einstein-relation (eqn (3) left), where η is the viscosity of the solvent, T the temperature, and k_B the Boltzmann constant.

The cumulant analysis provides a measure for the relative standard deviation σ_{rel} , here referred to as the polydispersity index, of an assumed Gaussian distribution from the relaxation rate Γ and the second moment of the distribution μ_2 :

$$R_h = \frac{k_B T}{6\pi\eta D_T} \text{ and } \sigma_{rel} = \sqrt{\frac{\mu_2}{\langle\Gamma\rangle^2}} \quad (3)$$

2.2.5. Small-angle neutron scattering (SANS). Small-angle neutron scattering (SANS) experiments on the systems TDMAO- $C_5F_{11}CO_2Li$ and TDMAO- $C_6F_{13}CO_2Li$ were performed on the

Table 1 Density ρ , scattering length density SLD, critical micelle concentration cmc and molecular weight M_w of the used surfactants

Molecular formula	$\rho/\text{g mL}^{-1}$	SLD/ nm^{-2}	$M_w/\text{g mol}^{-1}$	cmc/ mol L^{-1}
$\text{C}_{14}\text{H}_{39}(\text{CH}_3)_2\text{NO}$	0.897	-1.96×10^{-5}	257.46	1.2×10^{-425}
$\text{C}_5\text{F}_{11}\text{CO}_2\text{Li}$	2.019	4.25×10^{-4}	319.98	0.23 ²⁶
$\text{C}_6\text{F}_{13}\text{CO}_2\text{Li}$	1.947	4.11×10^{-4}	369.99	0.09 ²⁶
$\text{C}_7\text{F}_{15}\text{CO}_2\text{Li}$	1.922	4.07×10^{-4}	420.00	0.0334 ²⁷

instrument V4 of the Helmholtz-Zentrum Berlin (HZB) with neutrons of a wavelength of $\lambda = 6.05 \text{ \AA}$ with a FWHM of 10.5% at sample-detector distances of 0.975, 4, and 15.865 m and corresponding collimation lengths of 4, 8, and 16 m, respectively. The SANS-experiments on the system TDMAO-C₇F₁₅CO₂Li were performed on the instrument KWS-2 of JCNS (operating at FRMII, Munich) with neutrons of a wavelength of $\lambda = 4.7 \text{ \AA}$ with a FWHM of 20% at sample-detector distances of 1.4 and 8 m, and in addition, with neutrons of a wavelength of $\lambda = 11.8 \text{ \AA}$ with a FWHM of 20% at a sample-detector distance of 8 m and a collimation length of 8 m. All measurements were performed using Hellma quartz cuvettes with a cell thickness of 1 mm as sample containers.

The scattering intensities were detected on a 2-D ³He-detector at the V4 at HZB and on a ⁶Li-scintillation-detector at KWS-2 of JCNS. The 2-D images were corrected for the detector efficiency with water as a homogeneous scatterer for the measurements at the HZB and with water and Plexiglas for the measurements at KWS-2. At the HZB the attenuated direct beam was used to determine the transmissions and therefore the absolute intensities. At FRMII only the tail of the unattenuated direct beam was measured by a detector placed on top of the beamstop. This intensity was used to determine the transmissions and therefore the absolute intensities. The scattering intensity for the empty cell was subtracted and the two dimensional image was azimuthally averaged to obtain the scattering intensity as a function of q . These calculations were done using the data reduction software BerSANS.²⁸ The scattering length densities were determined by the Scattering Length Density Calculator provided by the NIST Center for Research (NIST).²⁹ The resulting scattering length densities employed are given in Table 1. The densities of diluted surfactant solutions with varying surfactant content were measured using an Anton-Paar DMA 4500 thermostatted at 25.00 °C. The pure surfactant density was determined by extrapolating the densities of the diluted solutions to a surfactant content of 100 wt% assuming additivity of the volumes of all components (Table 1). The scattering length densities for mixed aggregates were calculated as sums of the scattering length densities of the pure surfactants averaged with the volume fractions of the surfactants in the mixture (Table 1).

2.2.6. Cryo-scanning electron microscopy (Cryo-SEM). The samples were prepared with the sandwich technique. They were frozen in a copper sandwich sample holder in melting nitrogen. The sample in the sandwich sample holder was then broken to access the bulk phase and the broken surface was freeze-etched in a GATAN cryo transfer system. The samples were sputtered with Pt to gain a conductive coating. Field emission scanning electron microscopy was performed on a Hitachi S-4800 electron microscope at -145 °C.

3. Results and discussion

In the following we discuss first the interaction parameter between TDMAO and the various perfluoro surfactants as obtained from the determination of the cmc of the mixed micelles, then the phase behaviour of the mixtures as obtained from visual inspection, electric conductivity, pH, and viscosity measurements. DLS, FF-SEM, and SANS measurements were done in order to obtain a more refined structural picture. This is compared for systematic variations of the chain length of the perfluoro surfactant. In addition, we studied the effect of switching from a zwitterionic system to one in which 10% of the zwitterionic TDMAO was substituted by the cationic surfactant TDMAOH⁺Cl⁻. The advantage of the TDMAO is that it allows for a continuous switching from a zwitterionic to a catanionic surfactant mixture in a moderate pH-range of pH = 5–9. It should be noted that all the bilayer systems studied here were well above the chain melting temperature, *i.e.*, in a fluid state.

3.1. cmc-Measurements: Determination of the interaction parameter β

Our particular interest in this work was the formation of vesicles in zwitterionic mixtures as it arises from synergistic interactions between the two different surfactants. Perfluoro surfactants have a propensity to form bilayers due to their bulky alkyl chain.¹⁹ As we have a bilayer of mixed surfactants with largely different length of the alkyl chains one may expect the formation of asymmetric bilayers thereby facilitating vesicle formation. Such an asymmetry in chain length is frequently observed for the formation of unilamellar vesicles.^{4,30–32}

The tendency for formation of mixed aggregates for lithium perfluorocarboxylates and TDMAO is directly related to the interaction parameter β as it can be determined by cmc (critical micelle concentration) measurements. The cmc values of the pure surfactants (c_1 , c_2) and of surfactant mixtures (c^*) for different molar fractions α_1 of the surfactant 1 in the bulk were measured using conductivity detection (Fig. S.1 to S.7†) and the results are summarised in Fig. 1.

The interaction parameter was determined from the cmc values of the pure surfactants c_1 and c_2 and the mixed system c^* using the model from Holland and Rubingh.³³ Therefore eqn (4) was solved with an iterative method to calculate the molar fraction x_1 of surfactant 1 in the micelle.

$$\frac{x_1^2 \ln \left(\frac{c^* \alpha_1}{c_1 x_1} \right)}{(1-x_1)^2 \ln \left[\frac{c^* (1-\alpha_1)}{c_2 (1-x_1)} \right]} = 1 \quad (4)$$

With the molar fraction x_1 of the surfactant 1 in the mixed aggregates the interaction parameter β was calculated for all molar ratios α_1 according to:

$$\beta = \frac{\ln \left(\frac{c^* \alpha_1}{c_1 x_1} \right)}{(1-x_1)^2} \quad (5)$$

The mean value for β was determined and the results for the corresponding values for the theoretical cmc values according to the regular solution theory are plotted in Fig. 1.

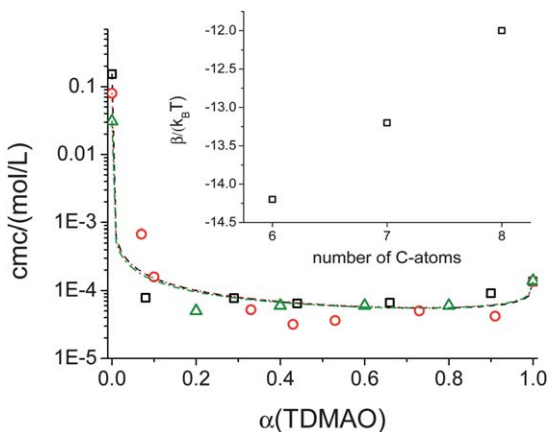


Fig. 1 Critical micelle concentration (cmc) determined by conductivity measurements; TDMAO- $C_5F_{11}CO_2Li$ measurement - □, theory with $\beta = -14.2$ - dashed line; TDMAO- $C_6F_{13}CO_2Li$ measurement - ○, theory with $\beta = -13.2$ - dotted line; TDMAO- $C_7F_{15}CO_2Li^{21}$ measurement - ▲, theory with $\beta = -12$ - dashed-dotted line; inset: average interaction parameter (β) for the synergistic interaction between TDMAO and perfluoro carboxylates as a function of the length of the anionic perfluoro surfactant.

The cmc* values are in the same order of magnitude for all three different mixed systems despite the fact that the cmc values for the three pure lithium perfluorocarboxylates strongly depend on the chain length and decrease with increasing number of C-atoms in the chain by about a factor of 2.5–3 per CF_2 group. That corresponds to a reduction of the Gibbs free energy of micellisation of $1.1 k_B T$ per CF_2 -group. The cmc-value for $C_5F_{11}CO_2Li$ and as a result the value of the change of the Gibbs free energy is lower than the value given by Moroi *et al.*,²⁶ but close to the value for $C_5F_{11}CO_2Na$ (cmc = 0.172 mM) given by Iampietro and Kaler.³⁴ This might be due to the different methods for cmc determination.

Apparently the synergistic interaction between the perfluoro surfactants and TDMAO is the stronger the shorter the perfluoro surfactant chain (Fig. 1). This is reasonable as the interaction of the perfluorinated chains with the hydrocarbon chains is unfavourable, while the head group interaction should basically be identically attractive. The interaction parameter β is reduced by $1.1 k_B T$ per CF_2 -group, describing the repulsion between hydrocarbon and fluorocarbon chains. The pronounced reduction of the Gibbs free energy in the mixed systems proves the pronounced synergistic interactions between the head groups of TDMAO and the anionic perfluoro carboxylates. In that context it might be noted that for the perfluorooctanoate in the catanionic mixture a value of $-21 k_B T$ has been reported.²¹ This means that by switching from a cationic-anionic (ion-ion interaction) to a zwitterionic-anionic (dipole-ion interaction) surfactant pair one reduces the attractive interaction of the head groups by about $9 k_B T$. According to these values of the interaction parameter, mixed aggregates will be formed and for such systems vesicle formation can be expected. Apparently the increase of the interaction parameter with growing chain length of the perfluoro surfactant just compensates the parallelly lower cmc's of the pure compounds as the c^* 's of the mixtures are quite similar.

3.2. Phase behaviour

As a first step we studied the macroscopic phase behaviour at $25^\circ C$ as a function of the mixing ratio for a given total surfactant concentration of 50 mM for mixtures of TDMAO with various anionic perfluoro surfactants of different chain lengths. In addition, we studied the case where TDMAO becomes slightly charged by protonation with HCl, thereby moving our system from a zwitterionic surfactant mixture to one that has catanionic properties. The phase behaviour of the mixtures was studied by visual inspection and further corroborated by means of measurements of electric conductivity, pH, viscosity, and hydrodynamic radius as determined by DLS.

The electric conductivity can be taken as an indication for vesicle formation. If vesicles are formed in the solution, a substantial part of the ions becomes entrapped, thereby reducing the ion mobility. Therefore the measured conductivity κ significantly deviates from the expected linear behaviour of the conductivity κ_0 with the composition α of a surfactant mixture without vesicles. From this reduced conductivity κ one can calculate the volume fraction of the contained vesicles, Φ_V , and the radius R of the vesicles can then be estimated from the volume fraction of the surfactant Φ_{amph} and the volume fraction of the vesicles Φ_V in the solution³⁵:

$$\Phi_V = \frac{1 - \frac{\kappa}{\kappa_0}}{\frac{\kappa}{\kappa_0} + 1} \quad (6)$$

$$R = \frac{3d\Phi_V}{\Phi_{\text{amph}}} \quad (7)$$

This calculation is valid under the assumption that the vesicles are unilamellar and monodisperse and that the vesicle radius is much larger than the thickness of the bilayer. The shell thickness d was determined from SANS measurements to be 2.3–2.7 nm (see later).

An increased viscosity could indicate formation of vesicles but this becomes only significant for volume fractions approaching dense packing. In contrast, a pronounced increase of viscosity can be expected for the case of formation of long cylindrical micelles already at low concentrations below or around 1 wt%.³⁶ Once they overlap the solutions become viscous and for still higher concentrations these micelles can form loose networks, where the knots in the network consist of entanglements of the micelles. They can be broken under shear stress but cause a high zero shear viscosity when the entanglements stay intact.³⁷ Whether vesicles or rod-like micelles are present can be further differentiated by means of DLS measurements, as vesicle formation leads to a pronounced increase of the hydrodynamic radius while the presence of cylindrical micelles leads only to moderately larger values.

3.2.1. TDMAO/ $C_5F_{11}CO_2Li$. First we studied the surfactant perfluorohexanoate with the shortest chain in order to see whether it is possible to form vesicles with such a rather weak amphiphile whose cmc is much higher than the concentration investigated here (see Table 1). All samples are clear and optically isotropic and the conductivity increases linearly with the amount

of ionic surfactant in the solution. This indicates the formation of micelles. The pH is higher in the mixtures than in the pure surfactant solutions (Fig. S.8†). This can be attributed to the fact that the presence of the anionic perfluoro surfactant stabilizes the protonation of the weakly basic amine oxide group and therefore enhances its degree of protonation, thereby raising the pH. This effect confirms the formation of mixed aggregates and is similarly observed for the longer chain analogues. The viscosity (Fig. 2) increases with increasing amount of perfluoro surfactant up to a maximum at $\alpha(\text{TDMAO}) = 0.5$ and decreases again for higher content of perfluoro surfactant. This indicates formation of rodlike micelles.

From DLS (Fig. 2) for the pure TDMAO solution a hydrodynamic radius R_h of 7.6 nm is observed (deduced from a cumulant analysis). Upon addition of perfluoro surfactant a decrease of R_h at $\alpha(\text{TDMAO}) = 0.9$ is observed, in agreement with the SANS measurements (see later). They show that the decrease of the hydrodynamic radius R_h , measured by DLS, arises from the fact that TDMAO forms cylindrical micelles with a length of 20 nm and the addition of small amounts of $C_5F_{11}CO_2Li$ leads to a decrease of the apparent R_h , which is presumably due to the charging effect. With further increase of the fraction of perfluoro surfactant the micelles apparently become elongated and form long cylindrical micelles which leads to a higher hydrodynamic radius again.

3.2.2. TDMAO/HCl/ $C_5F_{11}CO_2Li$. As the admixture of pure perfluorohexanoate does not lead to the formation of vesicles in zwitanionic mixtures with TDMAO, we were interested in seeing how a change towards a catanionic mixture might facilitate vesicle formation. For that purpose we charged the originally uncharged TDMAO by addition of HCl, thereby introducing cationic TDMAOH^+ into the system. Due to the fact that TDMAOH^+ is a weak acid with a pK_a -value of 5,³⁸ this is rather easily possible and for our investigation we chose a degree of charging of 10%, i.e. $c(\text{HCl})/c(\text{TDMAO}) = 0.1$. The addition of HCl reduces the pH of the TDMAO solution from 7.9 to 6. Upon admixture of perfluoro surfactant solution the pH rises again like in mixtures of the system TDMAO/ $C_5F_{11}CO_2Li$ (see Fig. S.9†). This rise in pH indicates again the formation of mixed aggregates and further protonation of TDMAO in the anionic environment of $C_5F_{11}CO_2Li$. The pH of the samples was not adjusted to

a fixed value, but the effective pK_a of the surfactant mixtures, and thereby the extent of protonation, will anyway depend on the mixing ratio. This means that the real degree of protonation of the TDMAO will be somewhat higher than the 10 mol% of added HCl. However, in total this effect will be rather small as can be estimated from the pH increase observed from pH ~6 to pH ~9, which corresponds to less than a relative change of 1% in the extent of the degree of protonation.

For $\alpha(\text{TDMAO}) = 1\text{--}0.9$ the samples were transparent and optically isotropic and the conductivity (Fig. 3) increases linearly with the perfluoro surfactant content, thereby indicating the formation of mixed micelles. At $\alpha(\text{TDMAO}) = 0.4\text{--}0.8$ a second lower turbid, flow birefringent phase of condensed large vesicles appears in addition to the micellar phase. In the range of $\alpha(\text{TDMAO}) = 0.1\text{--}0.3$ the samples are monophasic and show a bluish shimmer. In the turbid and the two-phase areas the conductivity (Fig. 3) is significantly lower compared to the linear behaviour, from which the presence of vesicles could be concluded.

DLS measurements (Fig. 3) confirm the presence of vesicles and the radii of 100–150 nm obtained from DLS and from conductivity measurements are similar in the mono- and biphasic region, the DLS data being more reliable. Comparing the phase behaviour of the systems TDMAO/ $C_5F_{11}CO_2Li$ and TDMAO/HCl/ $C_5F_{11}CO_2Li$ one observes that already the presence of this fairly small amount of 10 mol% cationic surfactant changes the aggregation behaviour of these systems drastically. The L_1 -phase, which is the only one present in the system TDMAO/ $C_5F_{11}CO_2Li$, is drastically reduced and formation of vesicles is induced due to stronger head group interactions between the cationic TDMAOH^+ and the anionic $C_5F_{11}CO_2^-$ thereby decreasing the packing parameter $p = v_S/(a_S l_S)$, where v_S is the volume of the hydrophobic part of the surfactant, a_S the head group area, and l_S the stretched length.³⁹

3.2.3. TDMAO/ $C_6F_{13}CO_2Li$. As a next step we increased the chain length of the anionic surfactant in order to see how this parameter influences the aggregation behaviour in the zwitanionic mixtures with TDMAO. For $\alpha(\text{TDMAO}) > 0.6$ a transparent, optically isotropic, micellar phase appears. From $\alpha(\text{TDMAO}) = 0.1\text{--}0.3$ the samples are transparent with a bluish

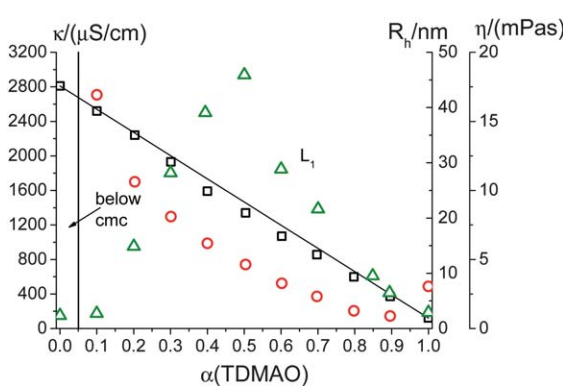


Fig. 2 TDMAO/ $C_5F_{11}CO_2Li$, 50 mM, $T = 25^\circ\text{C}$; conductivity (κ) \square , hydrodynamic radius (R_h) \bigcirc , and zero-shear viscosity (η_0) \triangle .

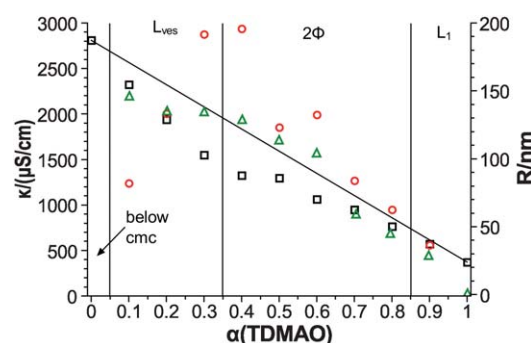


Fig. 3 TDMAO/HCl/ $C_5F_{11}CO_2Li$, 50 mM, $T = 25^\circ\text{C}$, $(c(\text{HCl})/c(\text{TDMAO})) = 0.1$; conductivity (κ) \square , and particle radius (R) determined by DLS measurements (hydrodynamic radius) \triangle and from the decrease of conductivity \bigcirc .

shimmer indicating the formation of vesicles. A two-phase area appears for $\alpha(\text{TDMAO}) = 0.4\text{--}0.6$ after a time of two weeks at 25 °C. The samples were optically isotropic and transparent directly after preparation. The upper phase is transparent and optically isotropic. The lower phase is white and shows flow birefringence. This lower phase only has a very small volume and presumably consists of a condensed vesicle phase (see Figs. S.12 and S.13†).

DLS experiments show an increase of the hydrodynamic radius R_h at the phase boundary between the micellar phase and the two-phase region (Fig. 4). In the micellar region R_h lies between 2 and 7 nm. The polydispersity calculated from the cumulant fit is quite high (see Fig. S.10† and Table S.1). At $\alpha(\text{TDMAO}) = 0.6$ close to the phase boundary in the two-phase area the intensity correlation function can better be described with a bi-exponential fit (see Fig. S.18†). One radius can be identified as the radius of micellar aggregates while the other radius is the hydrodynamic radius of large vesicles. The radii of the vesicles in the two-phase area lie between 75 and 165 nm. In the homogeneous vesicle area the aggregates are much more monodisperse and the vesicles are smaller. The vesicle radii lie between 50 and 60 nm which is in good agreement with the radii calculated from the decrease of the conductivity. The polydispersity is around 0.3 (see Table S.1†).

It is very interesting to note that the phase behaviour in this mixture is rather asymmetric. On the TDMAO rich side one starts from a micellar solution, where the rodlike micelles become increasingly longer until at a certain point the packing parameter has changed so much that bilayers are formed. This structural transition occurs *via* a two-phase situation. On the C₆F₁₃CO₂Li rich side one starts from a solution below the cmc but upon addition of TDMAO one immediately forms vesicles. Apparently the perfluoro surfactant here is below the cmc but its packing parameter is such that it forms bilayers easily and accordingly the first aggregate structure formed is directly that of vesicles. On the perfluoro surfactant rich side it can easily take up TDMAO to form vesicles while on the TDMAO rich side the TDMAO micelles incorporate the perfluoro surfactant. In the two-phase area the micelles and the vesicles do not have the same composition but the vesicles are rich in anionic perfluoro

surfactant and the micelles are rich in TDMAO. It is also interesting to note that the viscosity maximum occurs just upon entering the biphasic region from the TDMAO rich side (Fig. 4), as the largest amount of long rodlike micelles will be present.

3.2.4. TDMAO/HCl/C₆F₁₃CO₂Li. As before we studied the effect of changing from the purely zwitterionic system to a partly catanionic one by protonating the TDMAO by HCl to an extent of 10 mol%. The samples for $\alpha(\text{TDMAO}) = 0.1\text{--}0.5$ are all transparent with a bluish shimmer and low viscosity, *i.e.* here one has a largely extended vesicle region compared to the system without added HCl. The vesicle phase is shifted towards the TDMAO rich side. This is due to the packing parameter in mixtures with TDMAOH⁺, which is higher and favours bilayer formation. For the sample with $\alpha(\text{TDMAO}) = 0.5$ sedimentation was observed. A broad two-phase area for $\alpha(\text{TDMAO}) = 0.5\text{--}0.9$ is observed, with a transparent optically isotropic upper micellar phase and a turbid flow birefringent lower phase consisting of condensed vesicles. In the turbid areas and in the two-phase areas the conductivity is decreased compared to the linear interpolation of the conductivity from the pure surfactant solutions (Fig. 5). This decrease was even stronger than that in the system without TDMAOH⁺ (Fig. S.8†).

From the decrease of the conductivity, vesicle radii between 60 and 170 nm were calculated (eqn (7) and Fig. 5) in good agreement with the DLS measurements. This structural picture is furthermore corroborated by the cryo-SEM picture (Fig. 6) of the sample with $\alpha(\text{TDMAO}) = 0.5$ that shows spherical objects with a diameter of about 120–180 nm. Compared to the pure zwitterionic system already the addition of 10 mol% HCl leads to a pronounced enlargement of the vesicle phase and a substantial shift towards the TDMAO rich side of the phase diagram, thereby almost completely suppressing the L_1 -phase.

3.2.5. TDMAO/C₇F₁₅CO₂Li. The system TDMAO-C₇F₁₅CO₂Li was previously analysed by us²¹ and therefore shall only be briefly compared here to the counterparts with shorter perfluoro chains. The systems TDMAO-C₆F₁₃CO₂Li and TDMAO-C₇F₁₅CO₂Li show some similarities but as well some very important differences. Both systems show a vesicle area at low TDMAO content but in comparison the vesicle area is

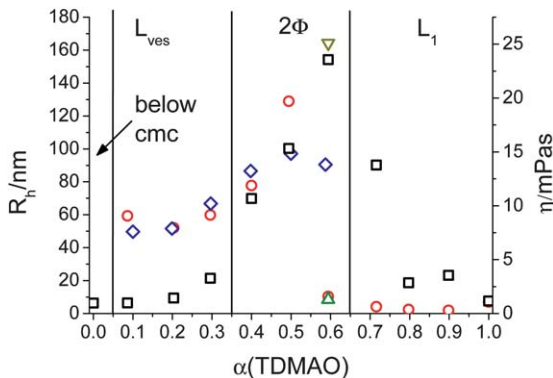


Fig. 4 TDMAO/C₆F₁₃CO₂Li, 50 mM, $T = 25$ °C; viscosity (η) □, hydrodynamic radius (R_h) determined with cumulant analysis ○ and for $\alpha(\text{TDMAO}) = 0.6$ with a bi-exponential fit of $g^{(2)}$ ▲ and ▼, and vesicle radius determined from the decrease of the conductivity ◇.

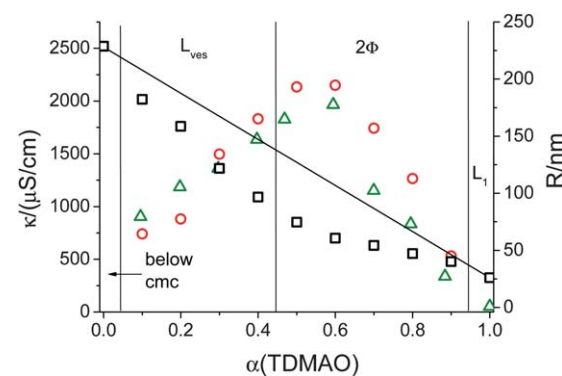


Fig. 5 TDMAO/HCl/C₆F₁₃CO₂Li, 50 mM, $T = 25$ °C; conductivity (κ) □, and particle radius (R) determined by DLS measurements (hydrodynamic radius) ▲ and from the decrease of conductivity ○.

Published on 17 October 2011. Downloaded by TU Berlin - Universitaetsbibliothek on 01/04/2016 09:38:02.

moved to larger fractions of TDMAO and is found for α (TDMAO) = 0.2–0.6 in the system with $C_7F_{15}CO_2Li$. In contrast to the system with $C_6F_{13}CO_2Li$ for lower α (TDMAO) = 0–0.1 micellar solutions of low viscosity are observed, where short cylindrical or nearly spherical micelles are present, and for higher α (TDMAO) > 0.6 no two-phase area is observed. So far it remains unclear why no macroscopic phase separation is observed, but it was verified that it neither occurs for extended periods of waiting nor upon centrifugation. The size of the vesicles determined by DLS varies between 25 and 80 nm. The radii obtained from the decrease of the conductivity are larger as determined by the DLS measurements. Like in the system with $C_6F_{13}CO_2Li$ at higher molar ratios of α (TDMAO) > 0.6 a second micellar region with higher viscosity can be found. The zero-shear viscosity reaches a maximum at α (TDMAO) = 0.7 with 33.2 mPa s close to the phase boundary (Fig. 7). Accordingly here, similar as in the systems TDMAO- $C_5F_{11}CO_2Li$ and TDMAO- $C_6F_{13}CO_2Li$, at higher TDMAO content networks of long cylindrical micelles are present.

3.3. Small angle neutron scattering (SANS)

In order to obtain a more detailed picture regarding the mesoscopic structural progression in the mixtures of zwitterionic TDMAO with anionic perfluoro surfactants of different chain length SANS measurements were performed as a function of the mixing ratio.

Pure TDMAO is known to form short cylindrical micelles at the given concentration.^{40,41} An analysis of our data with a model for polydisperse cylindrical micelles with a cylinder radius R and a log-normal distributed cylinder length with the mean length L and the polydispersity σ_{rel} (eqn S.4†) yields a length of cylinders of about 20 nm and a radius of 1.8 nm. These values are in good agreement with previous SANS work from Gorski and Kalus.⁴²

3.3.1. TDMAO/ $C_5F_{11}CO_2Li$. SANS experiments confirm, that at 50 mM total concentration in the whole mixing range of the system TDMAO- $C_5F_{11}CO_2Li$ cylindrical micelles are present

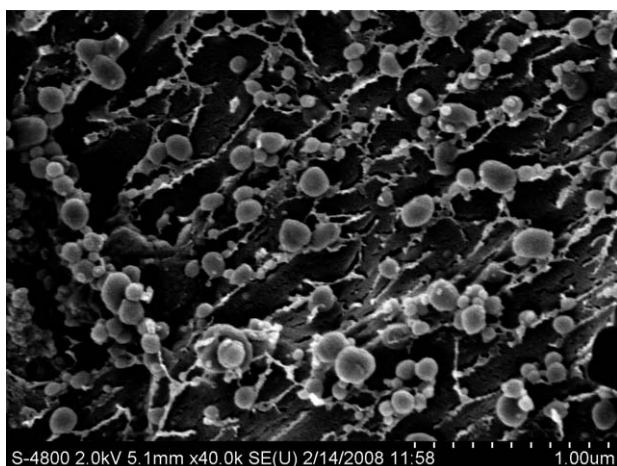


Fig. 6 Cryo-SEM micrograph of a mixture of TDMAO- $C_6F_{13}CO_2Li$ with 50 mM, α (TDMAO) = 0.5 and $c(HCl)$ = 2.5 mM; mostly vesicles with a radius of 140 nm are formed.

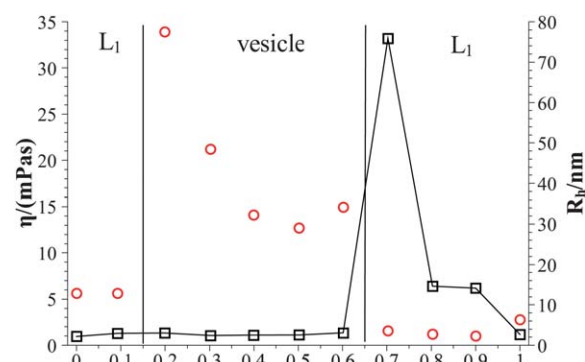


Fig. 7 TDMAO/ $C_7F_{15}CO_2Li$, 50 mM, T = 25 °C; hydrodynamic radius (R_h) (○) and viscosity (η) (□).

except for very low TDMAO content, where no micelles are formed (Fig. 8a).

Pure TDMAO micelles show no interaction peak but the addition of small amounts of $C_5F_{11}CO_2Li$ already leads to a repulsion between the micelles, which is visible as a correlation peak, thereby indicating the incorporation of the $C_5F_{11}CO_2Li$ and the formation of mixed micelles. The repulsive electrostatic interaction of the micelles becomes stronger with increasing content of $C_5F_{11}CO_2Li$. The SANS data were described with a model of interacting cylindrical micelles for which the scattering intensity as an approximation can be written as:

$$I_{\text{cylinder}, \text{RPA}}(q) = I_{\text{cylinder}}(q) \cdot S(q) \quad (8)$$

where $I_{\text{cylinder}}(q)$ is the scattering intensity for polydisperse cylindrical micelles (eqn S.4†). $S(q)$ is the structure factor that accounts for inter-particle interferences (eqn S.10†). In our case we employed for $S(q)$ an approximation based on the well-known hard sphere Percus–Yevick approximation⁴³ and modified for electrostatic repulsion described by a classical DLVO potential in a random phase approximation (RPA),⁴⁴ as it has been employed successfully before for the description of charged mixed micelles.⁴⁵ The additional parameters introduced by $S(q)$ are the effective electrostatic potential (ζ -potential), and the effective hard-sphere radius R_{eff} , while the particle number density for the structure factor was fixed by the volume fraction of amphiphilic material and the form factor. The fit parameters are summarised in Table 2 and it is interesting to note that the electrostatic potential increases with increasing TDMAO content up to 55 mV due to the decreasing concentration of Li and weaker counterion binding. The electrostatic repulsion in the pure TDMAO micelles is only caused by the slight protonation of the TDMAO and therefore at 11 mV is significantly lower than for the mixed micelles.

The fit parameters show that the cylinder length increases with increasing amount of $C_5F_{11}CO_2Li$ in the mixture, while the radius decreases. This is due to the increasing head group interactions and the increasing amount of short but bulky perfluoro surfactant chains, thereby increasing the packing parameter and decreasing the radius. That causes an increasing slope at low q which compensates the influence of the structure factor. For that reason the structure factor seems to vanish at low q with decreasing α (TDMAO). Due to the limited q -range the length of

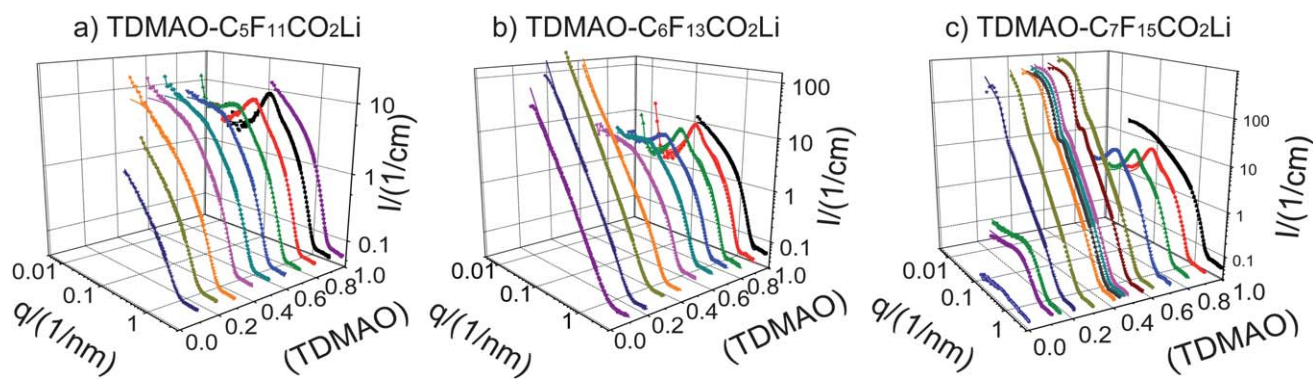


Fig. 8 Small angle neutron scattering (SANS) measurements of mixtures of TDMAO with various perfluoro surfactants (50 mM, 25 °C), a) $\text{C}_5\text{F}_{11}\text{CO}_2\text{Li}$, b) $\text{C}_6\text{F}_{13}\text{CO}_2\text{Li}$, c) $\text{C}_7\text{F}_{15}\text{CO}_2\text{Li}$. For TDMAO- $\text{C}_5\text{F}_{11}\text{CO}_2\text{Li}$ and TDMAO- $\text{C}_6\text{F}_{13}\text{CO}_2\text{Li}$ at $\alpha(\text{TDMAO}) = 0$, no measurement is shown since here one is below the cmc, 2-dimensional plots are given in the ESI (Figs. S.20 to S.22†).

the cylinders could not be determined for $\alpha(\text{TDMAO}) < 0.4$. The cylinder length for those measurements was fixed to a value of 40 nm as an upper limit of detection in our experiment. The elongation of the micelles correlates for $\alpha(\text{TDMAO}) = 0.5\text{--}1$ with the increase in viscosity (see Fig. S.23†) and is due to entanglements of the cylindrical micelles.

The hydrodynamic radius calculated from the DLS measurements is in good agreement with the hydrodynamic radius calculated from the length L and the radius R of the cylinders as obtained from the SANS measurements *via*:⁴⁶

$$R_h = (1.0304 + 0.0193x + 0.06229x^2 + 0.00476x^3 + 0.00166x^4 + 2.66 \times 10^{-6}x^7) \cdot \sqrt[3]{\frac{3}{4}R_{\text{cyl}}^2 L} \quad (9)$$

$$\text{with } x = \ln\left(\frac{L}{2} R_{\text{cyl}}\right)$$

3.3.2. TDMAO/C₆F₁₃CO₂Li. In the system TDMAO-C₆F₁₃CO₂Li cylindrical micelles with repulsive interactions,

Table 2 SANS fit parameters for a model of cylindrical micelles with electrostatic repulsion modeled with the RPA structure factor in the system TDMAO-C₅F₁₁CO₂Li (50 mM, 25 °C, molar fraction of TDMAO $\alpha(\text{TDMAO})$, cylinder radius R , cylinder length L , aggregation number of micelles $N_{\text{agg,micelle}}$, hydrodynamic radius $R_{\text{h,SANS}}$ calculated from SANS-parameters, hydrodynamic radius $R_{\text{h,DLS}}$ determined from DLS, effective hard-sphere radius R_{eff} , and electrostatic potential ζ used in the RPA structure factor)

$\alpha(\text{TDMAO})$	R/nm	L/nm	$N_{\text{agg,micelle}}$	$R_{\text{h,SANS}}/\text{nm}$	$R_{\text{h,DLS}}/\text{nm}$	R_{eff}/nm	ζ/mV
1.0	1.8	20	428	6.7	7	4	10
0.9	1.9	14	351	5.6	2	7	55
0.8	1.9	16	399	5.9	3	8	53
0.7	1.9	27	735	8.8	6	8	49
0.6	1.9	30	839	9.3	8	7	37
0.5	1.8	40	1125	11	12	8	31
0.4	1.8	40	1282	12	15		
0.3	1.8	(40)	1176		20		
0.2	1.8	(40)	1258		27		
0.1	1.5	(40)	994		42		

resulting in a pronounced correlation peak (Fig. 8b), are observed for $\alpha(\text{TDMAO}) = 0.9\text{--}0.7$. This behaviour at high TDMAO content is similar to that of the system TDMAO-C₅F₁₁CO₂Li. The micelles are charged and show the same repulsive interaction and screening effect from the Li counterions.

The increasing content of perfluoro surfactant in the solution leads to structural changes. The length of the micelles increases (as evidenced from the increase of the scattering intensity at low q) and cylindrical micelles with a length of about 40 nm are formed, as obtained by fitting the experimental data with eqn S.4.† At the same time the polydispersity of the length of the cylindrical micelles increases. The elongation of the micelles correlates with the increase in viscosity and is apparently due to entanglements of the cylindrical micelles (Fig. S.23†). Here it is interesting to note that for a similar length of micelles the longer the perfluoro chain of the anionic surfactant the higher the viscosity. This can be explained by an increased thickness and stiffness of the cylindrical micelles with increasing length of the perfluoro chain. This results in a larger structural relaxation time of the system and correspondingly higher viscosity.

From the cylinder length and radius, obtained by SANS, the hydrodynamic radii of these cylinders were calculated, which are in good agreement with those from DLS (Table 3).

In the two-phase region at $\alpha(\text{TDMAO}) = 0.5$ the scattering curve shows a combination of cylindrical micelles and large spherical shells (*i.e.* vesicles). By SANS measurements the phase transition could be detected in the same area of the phase diagram as by DLS measurements and the scattering data was then described by a structural two-state system for which the scattering intensity is given by:

$$I(q) = A_1 \cdot I_{\text{cylinder}}(q) + (1 - A_1) \cdot I_{\text{ves}}(q) \quad (10)$$

When subdividing the scattering contributions from the micelles and the vesicles the total volume fraction was kept fixed to be the one of dispersed amphiphilic material and their relative content in the form of cylinders or vesicles is described by the parameter A_1 . Here $I_{\text{cylinder}}(q)$ and $I_{\text{ves}}(q)$ for polydisperse vesicles (spherical shells) with a log-normal distributed intermediate radius R with a mean radius R_0 and a relative standard deviation σ_{rel} are given by eqns S.4 and S.9†, respectively.

Table 3 SANS fit parameters for a model of cylindrical micelles with electrostatic repulsion and vesicles in the system TDMAO-C₆F₁₃CO₂Li (50 mM, 25 °C, molar fraction of TDMAO α (TDMAO), volume fraction of scattering material in micelles A_1 , cylinder radius R , cylinder length L , aggregation number of micelles $N_{\text{agg,micelle}}$, lamellar thickness of the vesicles d , hydrodynamic radius $R_{\text{h,SANS}}$ calculated from SANS-parameters, hydrodynamic radius $R_{\text{h,DLS}}$ determined from DLS, effective hard-sphere radius R_{eff} , and electrostatic potential ζ used in the RPA structure factor)

α (TDMAO)	A_1	R/nm	L/nm	$N_{\text{agg,micelle}}$	d/nm	$R_{\text{h,SANS}}/\text{nm}$	$R_{\text{h,DLS}}/\text{nm}$	R_{eff}/nm	ζ/mV
1.0	1	1.8	20	428	6.7	7	4.1	10	
0.9	1	1.9	10	246	4.4	1.8	7.7	58	
0.8	1	1.9	11	298	4.9	2.5	8.3	61	
0.7	1	1.9	17	471	6.4	4.1	8.5	48	
0.6	0.97	1.9	24	685	8.0	10	9.0	48	
0.5	0.95	1.8	33	926	9.7	130	9.4	42	
0.4	0.47	1.6	15	334	2.5	78			
0.3	0				2.4	60			
0.2	0				2.3	52			
0.1	0				2.4	59			

In mixtures with a high perfluoro surfactant content $0 < \alpha(\text{TDMAO}) < 0.4$ the scattering intensity follows a q^{-2} law that indicates the presence of locally planar structures. From the slope a thickness of the bilayer of $\sim 2.5\text{ nm}$ can be deduced. This value can be compared with twice the length of the TDMAO-chain estimated from the number of C-atoms n_C in the TDMAO-chain:⁴⁷

$$d = 2 \cdot (1.5 \text{ \AA} + 1.265 \text{ \AA} \cdot n_C) \quad (11)$$

This value of 3.6 nm is significantly higher than the thickness deduced from SANS measurements. This estimation only holds for fully stretched hydrocarbon chains but here we have to take into account that in the vesicle region TDMAO is only the minority component. Accordingly an interdigititation with the much shorter perfluoro chains takes place. d calculated from eqn (11) for this case would be 2.8 nm (length of TDMAO plus perfluoro surfactant), in good agreement with the experimental data.

The phase study and DLS indicate that for $0 < \alpha(\text{TDMAO}) < 0.4$ vesicles of a radius of 50 nm with a polydispersity index of ~ 0.3 are formed. The SANS measurements showed no minimum due to the high polydispersity of the vesicles. Therefore the vesicle radius could not be determined from the SANS measurements, due to its restricted q -range.

As observed before the hydrodynamic radii calculated from the radius and the length of the cylindrical micelles and from the DLS measurements are in good agreement for $\alpha(\text{TDMAO}) < 0.5$ (Table 3).

3.3.3. TDMAO/C₇F₁₅CO₂Li. SANS-measurements in the system TDMAO-C₇F₁₅CO₂Li (Fig. 8c) confirm the phase behaviour already published by us before.²¹ It should be noted that the samples studied were all about two days old, in difference to the previously published study in which the systems studied were typically four weeks old. This may lead to some differences as slow aging of the vesicles will occur, which leads to an increase of the average size with time. A vesicle phase is observed for $\alpha(\text{TDMAO}) < 0.2\text{--}0.6$, which is marked by

a scattering pattern with pronounced oscillations around $q = 0.1 \text{ nm}^{-1}$ as they are typical for spherical shells. A quantitative analysis with fitting of eqn S.9† to the experimental data yields vesicle radii of 27 to 40 nm and polydispersity indices of about 0.3 (see Table 4). This means that for the longest perfluoro surfactant one has much more well-defined unilamellar vesicles than for the shorter perfluoro counterparts.

The volume fraction of scattering material in the micelles (A_1) shows that at $\alpha(\text{TDMAO}) = 0.2$ micelles and vesicles are present at the same time in the solution (Table 4). However, a macroscopic phase separation could not be observed over a long time range and could also not be enforced by centrifugation.

Between $\alpha(\text{TDMAO}) = 0.05\text{--}0.15$ and $\alpha(\text{TDMAO}) = 0.65\text{--}1$ cylindrical and for $\alpha(\text{TDMAO}) = 0\text{--}0.2$ nearly spherical micelles are observed. The scattering patterns of repulsive micelles are similar to those of the shorter chain perfluoro surfactant but the oscillations become more pronounced with increasing content of C₇F₁₅CO₂Li, indicating a lower polydispersity. At high TDMAO content long cylindrical micelles are found. The length of these micelles increases with increasing C₇F₁₅CO₂Li content. The presence of long wormlike micelles close to the phase boundary is as well indicated by the increase of the viscosity that correlates with the cylinder length derived from the SANS-fits (see Fig. S.23†).

4. Comparative discussion and conclusion

The comparison of the phase diagrams of the three perfluoro surfactants with different chain length shows that the vesicle region in the phase diagram moves to smaller molar fractions of TDMAO with decreasing chain length of the perfluoro surfactant, vanishing completely for C₅F₁₁CO₂Li (Fig. 9). Only for the system with C₇F₁₅CO₂Li a second micellar phase at low TDMAO content exists, while for the shorter perfluoro surfactants at 50 mM total concentration one is below the cmc. For

Table 4 SANS fit parameters for a model of cylindrical micelles with electrostatic repulsion and vesicles with a log-normal distributed radius in the system TDMAO-C₇F₁₅CO₂Li (50 mM, 25 °C, molar fraction of TDMAO α (TDMAO), volume fraction of scattering material in micelles A_1 , cylinder radius R , cylinder length L , aggregation number of micelles $N_{\text{agg,micelle}}$, mean vesicle radius R_{vesicle} , lamellar thickness of the vesicles d , vesicle polydispersity index PDI_{vesicle}, effective hard-sphere radius R_{eff} , and electrostatic potential ζ used in the RPA structure factor)

α (TDMAO)	A_1	R/nm	L/nm	$N_{\text{agg,micelle}}$	$R_{\text{vesicle}}/\text{nm}$	d/nm	PDI _{vesicle}	R_{eff}/nm	ζ/mV
1	1	1.8	20	428				4.1	10
0.9	1	2.0	12	340				8.1	57
0.8	1	2.1	14	437				8.9	63
0.7	1	2.3	24	949				9.0	65
0.6	0				32	2.6	0.29		
0.55	0				32	2.7	0.19		
0.47	0				29	2.7	0.26		
0.45	0				28	2.6	0.28		
0.43	0				28	2.6	0.20		
0.4	0				29	2.5	0.26		
0.3	0				30	2.5	0.41		
0.21	0.41	3.3	2	278				2.1	0.31
0.14	1	1.8	6	204				0.9	52
0.1	1	1.8	6	227				0.7	63
0	1	1.2	1	13				2.6	98

$C_6F_{13}CO_2Li$ the vesicle area extends to the pure perfluoro surfactant solution. This means for the shorter chain perfluoro surfactants, which then are below the cmc, one observes directly the formation of unilamellar vesicles as the first aggregation state upon the admixture of TDMAO. For increasing chain length of the perfluoro surfactant one finds an increased tendency for bilayer formation. At the same time the polydispersity of the vesicles decreases, and for all cases unilamellar vesicles are observed.

The changes in the phase diagram can be explained by the change of the packing parameter with the perfluoro surfactant chain length. The bulkier the perfluoro surfactant chain the larger is the packing parameter of the TDMAO- $C_nF_{2n+1}CO_2Li$ pair and the higher is the tendency for vesicle formation. On the other hand a higher anionic perfluoro surfactant content in the micelle leads to an increased repulsive interaction of the head groups and to a decreasing packing parameter. This can explain why a second micellar phase can be observed at lower TDMAO content in the system TDMAO- $C_7F_{15}CO_2Li$, which is not found for TDMAO- $C_5F_{11}CO_2Li$ and TDMAO- $C_6F_{13}CO_2Li$. For the latter two cases the cmc of the pure perfluoro surfactant is too low so that the perfluoro surfactant can only be incorporated into the TDMAO micelles.

All vesicles formed are unilamellar and long-time stable. This can be attributed to the interaction parameter that has been shown to have a constant contribution of about $-20 k_B T$ for the head group and becomes less attractive by about $1.1 k_B T$ per CF_2 group in the perfluoro surfactant.

It is interesting to observe that a slight shift from the zwitanionic system with TDMAO to a more catanionic system containing 10 mol% TDMAOH⁺ (relative to the total amount of TDMAO) has a very substantial effect on the phase behaviour. The synergistic interactions and the tendency for vesicle formation become much more pronounced. For instance, for the shortest chain $C_5F_{11}CO_2Li$, that does not form any vesicles with TDMAO, a relatively extended vesicle region is observed upon HCl addition. A similar shift is observed for $C_6F_{13}CO_2Li$. A comparison between the systems TDMAO/HCl/ $C_5F_{11}CO_2Li$ and TDMAO/HCl/ $C_6F_{13}CO_2Li$ (Fig. 10) shows again the shift of the vesicle region to lower TDMAO contents for $C_5F_{11}CO_2Li$ compared to $C_6F_{13}CO_2Li$ and the influence of the volume of the perfluoro surfactant. Compared to the systems without HCl the effect of the chain length on the phase behaviour is less pronounced, as in general apparently the effect of the charging (moving from zwitanionic to catanionic) has a much more

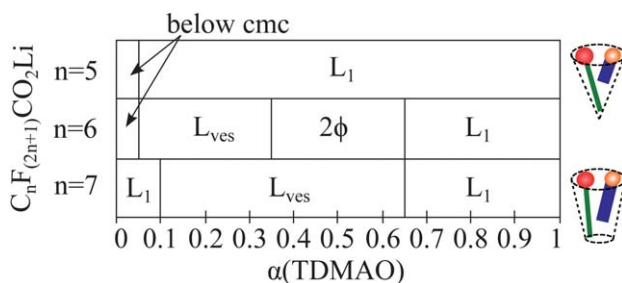


Fig. 9 Comparison of the phase behaviours of the systems TDMAO/ $C_nF_{2n+1}CO_2Li$ with $n = 5, 6, 7$, $c_{tot} = 50$ mM.

pronounced effect on the phase and structural behaviour compared to changing the alkyl chain length by one or two CF_2 groups.

An interesting point is that for the shorter perfluoro surfactants always a two-phase region is observed between the TDMAO rich micellar phase and the vesicle phase. This is observed with or without the addition of HCl but not for the case of the longer chain $C_7F_{15}CO_2Li$. This discrepancy is so far still unaccounted for.

Apparently the electrostatic conditions and chain length of the surfactants have a very pronounced effect on the packing parameter and therefore on the propensity of the given surfactant mixtures to form unilamellar vesicles. This all occurs in perfect agreement with the packing parameter paradigm.³⁹

In the systems TDMAO- $C_6F_{13}CO_2Li$ and TDMAO- $C_7F_{15}CO_2Li$ for a TDMAO content higher than in the vesicle phase, a region with cylindrical micelles is observed. The length of the micelles increases with decreasing amount of TDMAO in the solution and leads to an increased viscosity of the solutions. For the system TDMAO- $C_5F_{11}CO_2Li$ the maximum viscosity can be found in the middle of the phase diagram at $\alpha(TDMAO) = 0.5$, indicating that here the longest micelles are present. The maximum of the viscosity increases systematically with the chain length of the perfluoro surfactant. This may be due to an increase of the structural relaxation time that should be related to an increasing stiffness and thickness of the cylinders, and being in agreement with the SANS-measurements. In addition, the viscosity maximum shifts to higher TDMAO content with increasing chain length of the perfluoro surfactant.

In summary, it can be stated that zwitanionic surfactant mixtures composed of TDMAO and lithium perfluoro alkanoates are structurally versatile systems in which vesicle formation can be tuned by changing the chain length of the perfluoro alkanoate. Even stronger structural control can be exerted by changing the pH as already a relatively small degree of protonation of the TDMAO (thereby moving towards a catanionic system) affects the aggregation behaviour largely, transforming rod-like micelles directly to vesicles. This means that spontaneous formation of vesicles can be achieved by a proper choice of its composition and vesicle formation can easily be tuned by pH.

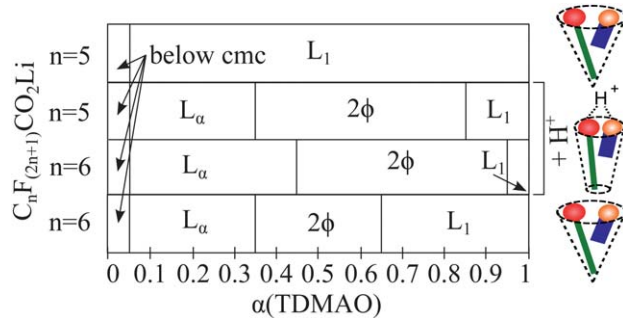


Fig. 10 Comparison of the phase behaviours of the systems TDMAO/HCl/ $C_nF_{2n+1}CO_2Li$ with $n = 5, 6$, influence of addition of HCl, $c_{tot} = 50$ mM.

Acknowledgements

This research work was financially supported by the German Research Council (DFG) within the frame of the priority program SPP 1273 Kolloidverfahrenstechnik (GR1030/7-1 and 2). The SANS measurements on V4 at the HZB have been supported by the European Commission under the 6th Framework Programme through the Key Action: Strengthening the European Research Infrastructures (Contract n°: RII3-CT-2003-505925 (NMI 3)). The SANS measurements on KWS-2 of JCNS (operating at FRMII, Munich) have been supported by the European Commission under the 7th Framework Programme through the ‘Research Infrastructures’ action of the ‘Capacities Programme’ Contract no.: 226507 (NMI3). M. G. would like to thank the Institute Laue-Langevin (ILL, Grenoble, France) and the DFG (project GR1030/10) for hospitality and funding of his sabbatical stay during which this manuscript was produced. Fruitful discussions with T. Narayanan are gratefully acknowledged. Finally we would like to thank the referees for their constructive comments that helped to improve the manuscript.

References

- M. Ambuehl, F. Bangerter, P. L. Luisi, P. Skrabal and H. J. Watzke, *Langmuir*, 1993, **9**, 36–38.
- M. Dubois, B. Deme, T. Gulik-Krzywicki, J.-C. Dedieu, C. Vautrin, S. Desert, E. Perez and T. Zemb, *Nature*, 2001, **411**, 672–675.
- H. Fukuda, K. Kawata, H. Okuda and S. L. Regen, *J. Am. Chem. Soc.*, 1990, **112**, 1635–1637.
- M. Gradzielski, *J. Phys.: Condens. Matter*, 2003, **15**, R655–R697.
- K. L. Herrington, E. W. Kaler, D. D. Miller, J. A. Zasadzinski and S. Chirivolu, *J. Phys. Chem.*, 1993, **97**, 13792–13802.
- N. Kamenka, M. Chorro, Y. Talmon and R. Zana, *Colloids Surf.*, 1992, **67**, 213–222.
- E. W. Kaler, K. L. Herrington, A. K. Murthy and J. A. N. Zasadzinski, *J. Phys. Chem.*, 1992, **96**, 6698–6707.
- H. T. Jung, B. Coldren, J. A. Zasadzinski, D. J. Iampietro and E. W. Kaler, *Proc. Natl. Acad. Sci. U. S. A.*, 2001, **98**, 1353–1357.
- E. Marques, A. Khan, M. da Graca Miguel and B. Lindman, *J. Phys. Chem.*, 1993, **97**, 4729–4736.
- C. Vautrin, M. Dubois, T. Zemb, S. Schmoelzer, H. Hoffmann and M. Gradzielski, *Colloids Surf., A*, 2003, **217**, 165–170.
- E. F. Marques, O. Regev, A. Khan, M. da Graca Miguel and B. Lindman, *J. Phys. Chem. B*, 1998, **102**, 6746–6758.
- S. Safran, F. MacKintosh, P. Pincus and D. Andelman, *Prog. Colloid Polym. Sci.*, 1991, **84**, 3–7.
- W. Guo, E. K. Guzman, S. D. Heavin, Z. Li, B. M. Fung and S. D. Christian, *Langmuir*, 1992, **8**, 2368–2375.
- G. Martini, S. Ristori and S. Rossi, *J. Phys. Chem. A*, 1998, **102**, 5476–5480.
- S. Rossi, G. Karlsson, S. Ristori, G. Martini and K. Edwards, *Langmuir*, 2001, **17**, 2340–2345.
- J. Hao, H. Hoffmann and K. Horbaschek, *Langmuir*, 2001, **17**, 4151–4160.
- T. Weiss, T. Narayanan and M. Gradzielski, *Langmuir*, 2008, **24**, 3759–3766.
- H. Watzke, *Prog. Colloid Polym. Sci.*, 1993, **93**, 15–21.
- N. Boden, J. Clements, K. Jolley, D. Parker and M. Smith, *J. Chem. Phys.*, 1990, **93**, 9096–9106.
- H. Iijima, T. Kato, H. Yoshida and M. Imai, *J. Phys. Chem. B*, 1998, **102**, 990–995.
- C. Wolf, K. Bressel, M. Drechsler and M. Gradzielski, *Langmuir*, 2009, **25**, 11358–11366.
- T. M. Weiss, T. Narayanan, C. Wolf, M. Gradzielski, P. Panine, S. Finet and W. I. Helsby, *Phys. Rev. Lett.*, 2005, **94**, 038303.
- K. Bressel, M. Muthig, S. Prevost, I. Grillo and M. Gradzielski, *Colloid Polym. Sci.*, 2010, **288**, 827–840.
- J. Gummel, M. Sztucki, T. Narayanan and M. Gradzielski, *Soft Matter*, 2011, **7**, 5731–5738.
- H. Hoffmann and G. Pössnecker, *Langmuir*, 1994, **10**, 381–389.
- Y. Moroi, M. Takeuchi, N. Yoshida and A. Yamauchi, *J. Colloid Interface Sci.*, 1998, **197**, 221–229.
- R. Muzzalupo, G. A. Ranieri and C. Lamesa, *Colloids Surf., A*, 1995, **104**, 327–336.
- U. Keiderling, *Appl. Phys. A: Mater. Sci. Process.*, 2002, **74**, 1455–1457.
- A. Munter, *Scattering Length Density Calculator*, 11/2/2010, <http://www.ncnr.nist.gov/resources/sldcalc.html>.
- L. L. Brasher and E. W. Kaler, *Langmuir*, 1996, **12**, 6270–6276.
- S. R. Raghavan, G. Fritz and E. W. Kaler, *Langmuir*, 2002, **18**, 3797–3803.
- M. E. Nabi, *Investigations on the Behaviour and Properties of Different Types of Unilamellar Vesicles*, Dissertation, 2006, Universität Bayreuth, Germany.
- P. M. Holland and D. N. Rubingh, *J. Phys. Chem.*, 1983, **87**, 1984–1990.
- D. Iampietro and E. Kaler, *Langmuir*, 1999, **15**, 8590–8601.
- U. Olsson, K. Nakamura, H. Kunieda and R. Strey, *Langmuir*, 1996, **12**, 3045–3054.
- H. Rehage and H. Hoffmann, *Mol. Phys.*, 1991, **74**, 933–973.
- M. E. Cates and S. J. Candau, *J. Phys.: Condens. Matter*, 1990, **2**, 6869–6892.
- S. A. Lawrence, *Amines: synthesis, properties and applications*, Cambridge University Press, The Edinburgh Building, Cambridge, CB2 2RU, UK, 2004, p. 371.
- J. N. Israelachvili, D. J. Mitchell and B. W. Ninham, *Biochim. Biophys. Acta, Biomembr.*, 1977, **470**, 185–201.
- H. Hoffmann, G. Oetter and B. Schwandner, *Prog. Colloid Polym. Sci.*, 1987, **73**, 95–106.
- H. Pilsl, H. Hoffmann, S. Hofmann, J. Kalus, A. W. Kencono, P. Lindner and W. Ulbricht, *J. Phys. Chem.*, 1993, **97**, 2745–2754.
- N. Gorski and J. Kalus, *J. Phys. Chem. B*, 1997, **101**, 4390–4393.
- N. W. Ashcroft and J. Lekner, *Phys. Rev.*, 1966, **145**, 83–90.
- L. Baba-Ahmed, M. Benmouna and M. J. Grimson, *Phys. Chem. Liq.*, 1987, **16**, 235–238.
- N. Gorski, M. Gradzielski and H. Hoffmann, *Langmuir*, 1994, **10**, 2594–2603.
- S. Hansen, *J. Chem. Phys.*, 2004, **121**, 9111–9115.
- C. Tanford, *J. Phys. Chem.*, 1972, **76**, 3020–3024.